Unveiling the nature of the intriguing source X Persei: A deep look with a *Suzaku* observation

Chandreyee Maitra, Laboratoire AIM, IRFU/Service d'Astrophysique, France
Harsha Raichur, NORDITA, Roslagstullsbacken 23, SE-10691 Stockholm, Sweden
Pragati Pradhan, St. Josephs College, Singamari, Darjeeling-734104, West Bengal, India
Biswajit Paul, Raman Research Institute, Sadashivnagar, Bangalore-560080, India

Abstract

We present detailed broadband timing and spectral analysis of the persistent, low luminosity and slowly spinning pulsar X Persei using a deep Suzaku observation of the source. The spectrum is unusually hard with a cyclotron resonance scattering feature (CRSF) at $\sim$ 30 keV, the presence of which has been debated. We have obtained the best constraint on the broadband spectral model of X Persei obtained so far. In addition we confirm the presence of a CRSF at 31 keV, hence providing an estimate of the magnetic field at 2.6×10^{12} G. We have identified for the first time, the presence of different intensity states in the source with distinct changes in the pulse profile and energy spectrum indicating changes in the accretion geometry. We have also found evidence of a positive correlation of the CRSF centroid energy with intensity consistent with accretion in the subcritical regime.

1 Introduction

X Persei (4U 0352 + 309) is a binary system at a distance of $\sim$ 0.95 kpc (Telting et al. 1998) that comprises a neutron star and a Be-star as its companion (Lyubimkov et al. 1997). The neutron star in this binary system has a very long period of $\sim$ 837 s (White et al. 1976). The orbit is wide with an eccentricity of $\sim$ 0.11 and a periodicity of $\sim$ 250 d (Delgado-Marti et al.2001). Unlike other Be X-ray binaries that show Type I outbursts during the periastron passage, X Persei does not exhibit such outbursts, probably because the neutron star is far away from the optical companion (Delgado-Marti et al. 2001). This makes it a persistent Be X-ray binary, however with a luminosity higher than other similar systems ($\sim 10^{35}$ erg/s). The measured X-ray luminosity rules out accretion from a fast and low-density stellar wind and instead favors accretion being from a slow dense wind probably originating from an equatorial disc of its companion. The absence of regular outbursts from X Persei during it's perisatron passage is hence intriguing. The X-ray spectrum of X Persei is also unlike most accreting X-ray pulsars, which can be modeled with a power-law and a cutoff in the range 10-30 keV (White, Swank & Holt 1983). X Persei has an unusually hard X-ray spectrum which can be fit with a two component model comprising two power laws with exponential cutoffs where one dominates at low energies and the other at higher energies (Di Salvo et al. 1998). A hard X-ray tail in the spectrum of X Persei is also reported in some instances (Robba et al. 1996). The *RXTE* spectrum is described by a blackbody at low energies (with kT $\sim$ 1.8 keV) and a power law with a broad absorption feature $\sim$ 30 keV which has been attributed a CRSF (Coburn et al. 2001). The presence of the CRSF however was not found previously in the BeppoSAX observation (Di Salvo et al. 1998), nor was it confirmed subsequently in the INTEGRAL data (Doroshenko et al. 2012). Hence there is no clear agreement on the unusual nature of the X-ray spectrum of the source, both with respect to the continuum model and the presence of the CRSF.

2 Observation & Analysis

The results reported here are from the analysis of a long (153 ks) observation of X Persei with *Suzaku*. *Suzaku* is a broadband X-ray observatory covering an energy range of 0.2-600 keV. The two main instruments on board are (i) the X-ray Imaging Spectrometer (XIS: covering 0.2-12 keV) (ii) the Hard X-ray Detector (HXD: PIN diodes covering the range of 10-70 keV and GSO crystal scintillators detectors covering 70-600 keV).

The data was reduced and processed with the standard procedures and using the latest CALDB version. XIS data was examined for the presence of pile-up. A central region corresponding to a pile-up fraction > 4 % was discarded from the analysis. Pulsations were found in the light curve at 835.28 s from epoch-folding technique, which was subsequently used to fold the light curves to create the pulse profiles. Figure 1 a. shows the light curves in the low (XIS: 0.2-12 keV) and high (PIN: 10-70 keV) energy band along with the hardness ratio (HR), binned at the spin period of the source. The count rates in both the energy bands vary by a large factor during the observation. Moreover the HR shows a strong variation with the PIN count rate (see Figure 1 b.) which indicates spectral variability in the source. In order to construct a model of the representative X-ray spectrum of the source, it is important to choose a time interval free from intensity or spectral variations. Therefore, a stretch of the observation (HR: 0.01-0.03 and PIN c/s-0.8-1.4) was chosen, where the dependence of HR with PIN count rate is linear.

The energy spectrum was modeled phenomenologically with different continuum models used to fit the spectra of accretion powered pulsars like the power law with high energy cutoff (highecut, newhcut), or power law with the Fermi Dirac cutoff (fdcut), the cutoff power law (cutoffpl) model, the negative-positive exponential power law component (NPEX), or the thermal comptonization model 'CompTT' and 'COMPMAG' which describes the spectral formation in the accretion column taking into account both thermal and Bulk Motion Comptonization. All the models are available as a standard package in *XSPEC*.

3 Broad band spectroscopy

With the broadband sensitive instruments on board *Suzaku*, we have obtained the best-constrained spectral model of X Persei till date. As in the previous works using the BeppoSAX (Di Salvo et al. 1998), *RXTE* (Coburn et al. 2001) and *INTEGRAL* (Doroshenko et al. 2012) observations, a two component model is required to fit separately the low and the high energy part of the broadband *Suzaku* spectrum (using XIS+PIN+GSO). We tried to fit the broadband spectrum with all the continuum models mentioned in section 2. For all the continuum models, a broad absorption feature (~ 30 keV) was evident in the residuals, reminiscent of the CRSF reported from *RXTE* observations. Accounting for a CRSF absorption profile ('cyclabs' in *XSPEC*) improves the fit significantly. The probability of chance improvement (PCI) for the CRSF inclusion is 0.5 % using a Run-test. Another important point is that since the spectrum of X Persei is unusually hard and extends > 100 keV, the GSO spectrum is crucial to constrain the cutoff in the high energy range, as it mostly appears to be a hard tail like feature in the PIN band (10-70 keV). Overall, we find a two component power law model with exponential rollover as the best representative continuum model of the X-ray spectrum of X Persei, since it gives the best-fit quality as well as the best-constrained CRSF feature. Table 1 summarizes the best-fit broadband spectral parameters obtained using the 'newhcut' (power law with smoothed exponential cutoff) model, and Fig 3. the best-fit continuum spectrum. The best-fit continuum parameters we obtain are consistent with the results obtained using BeppoSAX observation. However, *Suzaku* being more sensitive then the former at the high energy range, the high energy parameters are better constrained. The CRSF is obtained at the same energy reported by Coburn et al. 2001 from *RXTE* observations. The line is however shallower and narrower than reported by Coburn et al. 2001.

Table 1: Best fitting phase averaged spectral parameters of X-per. Errors quoted are for 99 per cent confidence range.

parameters	NEWHCUT
$N_{\rm H}$ (10^{22} atoms cm^{-2})	0.47 ± 0.02
$\Gamma_1(lowenergy)$	0.30 ± 0.08
E1-folding energy (keV)	3.57 ± 0.2
E1-cut energy (keV)	2.94 ± 0.04
Γ_2 (high energy)	1.57 ± 0.02
E2-folding energy (keV)	23.6 ± 15
E2-cut energy (keV)	57.9 ± 10
CRSF D_0	0.20 ± 0.08
CRSF E_0 (keV)	31.3 ± 2.1
CRSF W_0 (keV)	6.6 ± 3.0
Flux (XIS) [d] (0.3-10 keV)	$6.76 \times 10^{-10} \pm 0.12$
Flux (PIN) [e] (10-70 keV)	$7.43 \times 10^{-10} \pm 0.1$
reduced χ^2/d.o.f	1.64/553

4 Intensity states

The light curves of X Persei in both the low and high energy bands show large variations in the count rate. A large variation in the HR is also observed (see Figure 1). This motivated us to delve deep to look for intensity states in the source. Figure 2. shows the spin period averaged count rate histogram constructed from the combined XIS light curves. From the histogram, we identified four intensity states of the source as stated : Low state: Count rate $<$ 31 c/s, Int-1 state: 31 c/s $<$ Count rate $<$ 45 c/s, Int-2 state: 45 c/s $<$ Count rate $<$ 65 c/s, High state: Count rate $>$ 65 c/s. To investigate whether these are intrinsic spectral states associated with changes in the accretion geometry we investigated the pulse profiles and the broadband spectrum of the source at the different intensity states. The results are presented in the subsequent subsections.

4.1 Pulse profiles

Figure 4. shows the background subtracted pulse profiles of X Persei at different intensity states constructed from XIS (0.5-10 keV), PIN (10-70 keV) and GSO (50-100 keV) light curves respectively. The pulse profiles exhibit noticeable evolution with intensity with the profiles becoming narrower at higher intensities with increasing pulse fraction. The pulse profile at the highest intensity state (in black) is narrow with a pulse fraction around 60 %. This points towards a change in the accretion geometry and a gradual evolution in the beaming pattern with increasing intensity.

4.2 Energy spectrum

The spectrum of X Persei in tune with the pulse profiles, show distinct evolution with the intensity states. Figure 3. shows the spectrum of X Persei at different intensity states compared alongside the average spectrum. A noticeable change in the CRSF feature around $\sim$ 30 keV is seen. The CRSF feature is more prominent at higher intensity states (PCI for the CRSF inclusion decreases to 0.3 % for the high state). Moreover the CRSF is deeper and the centroid energies move to higher energies with increasing intensity. There is also a change in the power law slope with the spectrum getting harder with increasing intensity. All of these indicate distinct spectral states of the source and changes in the accretion geometry with change in the intensity. The harder spectrum at higher intensities (High and Int-2 state) may provide more seed photons for resonance scattering and hence be the cause of the presence of more prominent CRSF at these states. Table 2 tabulates the CRSF parameters and the power law index at the four intensity states. The CRSF width has been frozen to the average value at all of fits because of statistical limitations.

Table 2: Spectral parameters of X Persei at different intensity states. Errors quoted are for 99 per cent confidence range.

parameters	High	Int-2	Int-1	Low
Γ_2 (high energy)	1.45 ± 0.03	1.48 ± 0.02	1.55 ± 0.02	1.67 ± 0.04
CRSF E_0 (keV)	38.1 ± 1.8	38.5 ± 1.5	31.5 ± 2.0	33.4 ± 6.1
CRSF D_0	0.7 ± 0.1	0.4 ± 0.1	0.24 ± 0.07	0.26 ± 0.19

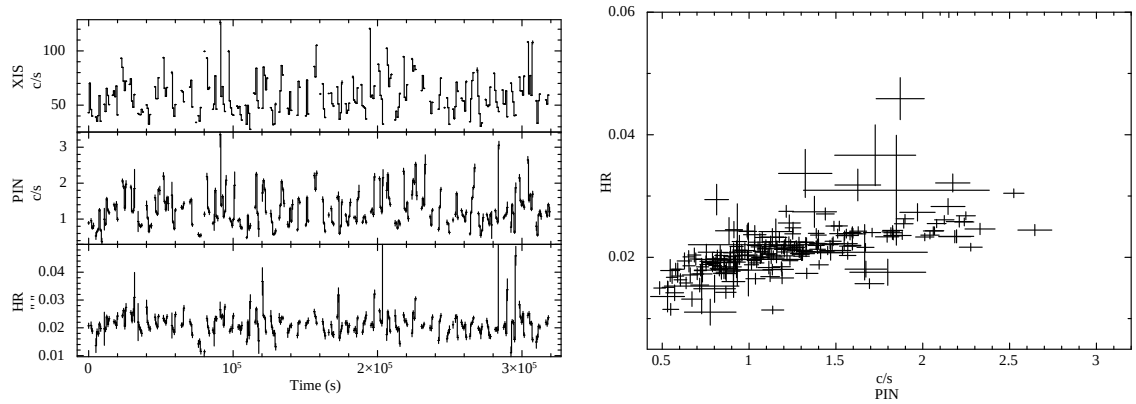

(a) (b)

Figure 1: Left figure shows the light curves in low and high energy bands with the lowest panel showing the hardness ratio. The light curves are binned at 835.28 s. Right figure shows the HR plotted against the PIN count rate to highlight the variation in HR with the count rate in the high energy band.

5 CRSF variation with intensity

The CRSF centroid energy is expected to evolve with intensity, linked to the changes in the location of the line forming region, and also the effect of increasing radiation pressure with increasing intensity (Becker at al. 2012, Mushtukov et al. 2015). Sources in the super-critical regime (exhibiting super Eddington luminosity locally) like V 0332+53 and 4U 0115+63 exhibit a negative correlation of the CRSF centroid energy with intensity, whereas sources in the sub-critical regime like Her X-1 and GX 304-1 exhibit a positive correlation of the CRSF centroid energy with intensity. X Persei with a luminosity of 2 $\times 10^{35}$ erg/s (0.5-70 keV) is expected to be in the sub-critical regime. Figure 5. shows the variation of the CRSF centroid energy with intensity in X Persei. As already discussed in the previous section, the CRSF centroid moves to higher energies at higher intensities, thus exhibiting a positive correlation between the two. This is consistent with the predicted scenario of changes in the accretion geometry and the line forming region with intensity (Becker at al. 2012).

6 Summary

We present the most detailed broadband timing and spectral study of X Persei performed so far. By testing different continuum models, we have obtained the best representative X-ray spectrum of X Persei till date. We have also confirmed the presence of a CRSF at $\sim$ 31 keV hence providing an estimate of the magnetic field at 2.6×10^{12} G. For the first time, we have identified different intensity states of the source with distinct changes in the pulsation characteristics and the energy spectrum. All of these indicate a change in the accretion geometry of X Persei with varying intensity. We have also found evidence that the CRSF is more prominent a higher intensities. Moreover, the CRSF centroid energy exhibits a positive correlation with intensity consistent with the scenario of accretion in a sub-critical regime.

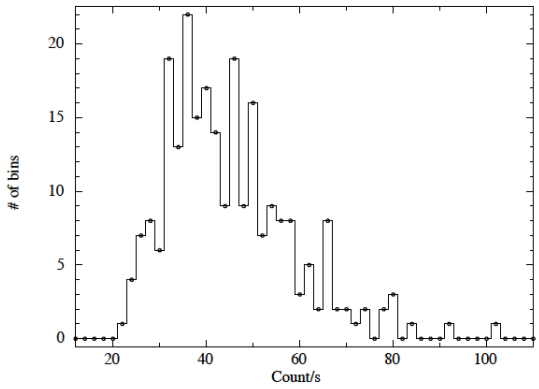

Figure 2: Spin period averaged count rate histogram constructed from the combined XIS light curves. From the histogram, we identified four intensity states of the source as stated : Low state: Count rate < 31 c/s, Int-1 state: 31 c/s $<$ Count rate < 45 c/s, Int-2 state: 45 c/s $<$ Count rate < 65 c/s, High state: Count rate > 65 c/s.

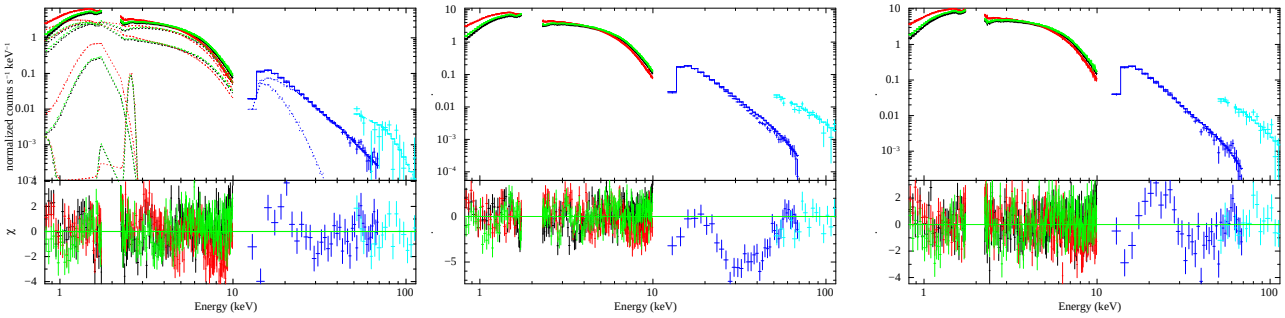

Figure 3: Leftmost figure: The upper panel shows the average (or representative) energy spectrum of X-Per showing the different continuum model components without the inclusion of the CRSF. The lower panel shows the residuals of the best fit model showing the presence of the CRSF. Middle and the leftmost figures show the same, for the Int-2 and high intensity states respectively. The spectral model components have been shown only for the average spectrum.

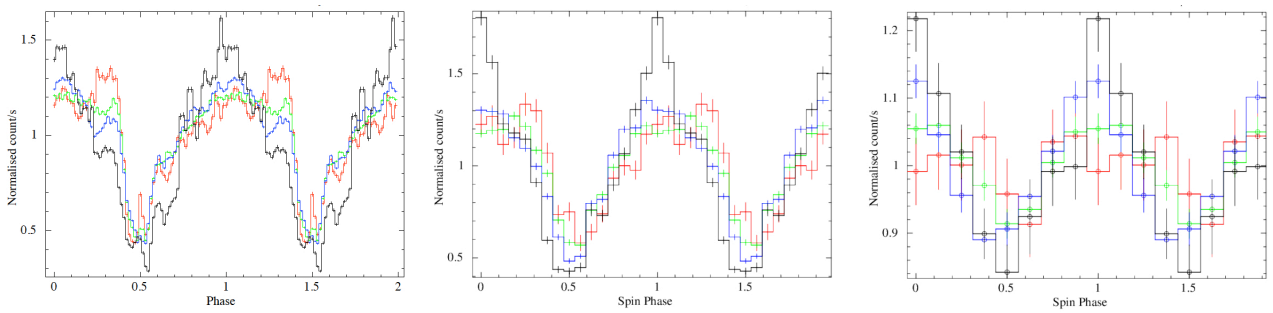

Figure 4: Intensity resolved pulse profiles constructed using XIS (left:0.5-10.0 keV), PIN (centre: 10-70 keV), and GSO (right: 50-100 keV). The pulse profiles in high, int-2, int-1 and low intensity states are shown in black, blue, green and red respectively.

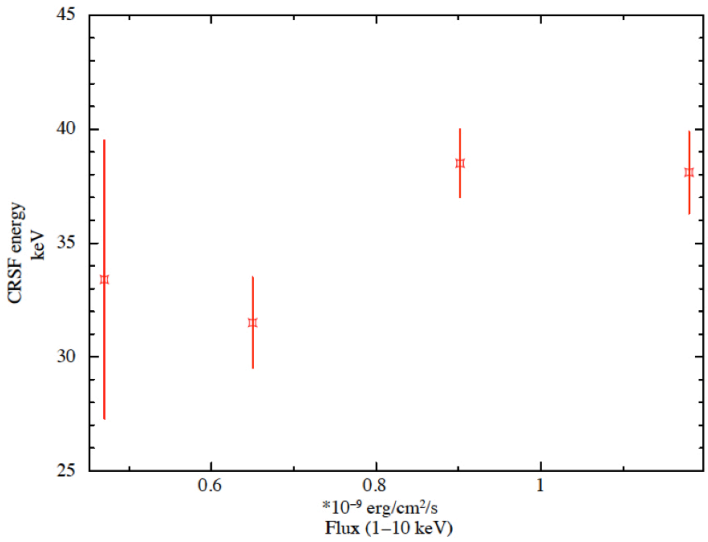

Figure 5: CRSF centroid energy plotted against the observed intensity states. A positive correlation is observed between the two.

References

[1] Becker, P. A., Klochkov, D., Schnherr, G., et al. 2012, A&A, 544, A123

[2] Coburn W., Heindl W. A., Gruber D. E., Rothschild R. E., Staubert R., Wilms J., Kreykenbohm I., 2001, ApJ, 552, 738

[3] Delgado-Marti H., Levine A. M., Pfahl E., Rappaport S. A., 2001, ApJ, 546, 455

[4] Di Salvo T., Burderi L., Robba N. R., Guainazzi M., 1998, ApJ, 509, 897

[5] Doroshenko V., Santangelo A., Kreykenbohm I., Doroshenko R., 2012, A&A, 540, L1

[6] Lyubimkov L. S., Rostopchin S. I., Roche P., Tarasov A. E., 1997, MNRAS, 286, 549

[7] Mushtukov, Alexander A., Tsygankov, Sergey S., Serber, Alexander V., Suleimanov, Valery F., Poutanen, J., 2015, MNRAS, 454, 2714

[8] Robba N. R., Warwick R. S., 1989, ApJ, 346, 469

[9] Telting J. H., Waters L. B. F. M., Roche P., Boogert A. C. A., Clark J. S., de Martino D., Persi P.,1998, MNRAS, 296, 785

[10] White N. E., Mason K. O., Sanford P. W., Murdin P., 1976, MNRAS, 176, 201